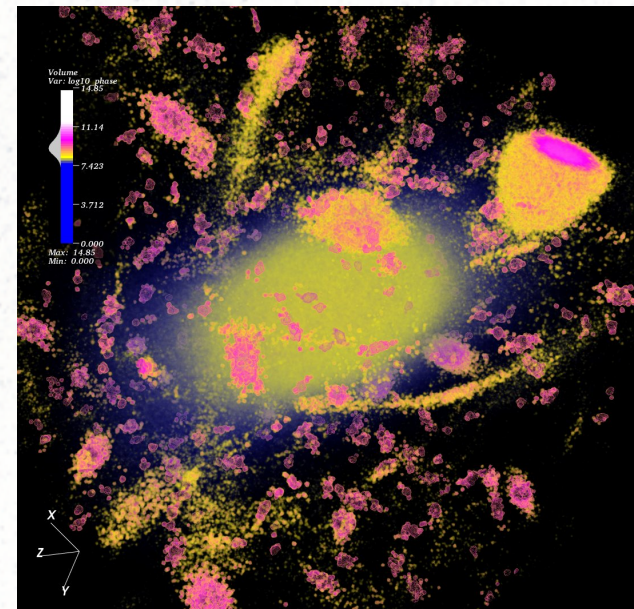
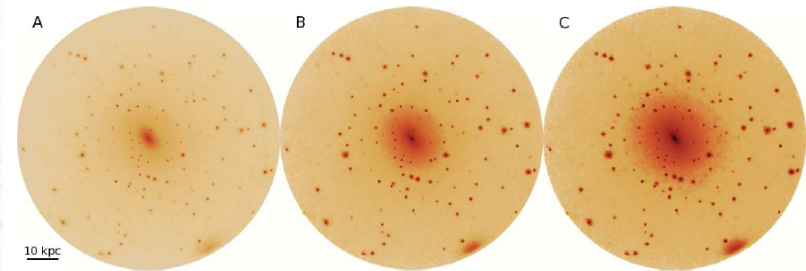


Galactic Substructure and Dark Matter Detection

Michael Kuhlen, UC Berkeley



The Via Lactea collaboration

(P. Madau, J. Diemand, M. Zemp, B. Moore, J. Stadel, D. Potter, V. Rashkov)

Galactic Substructure and Dark Matter Detection

Michael Kuhlen, UC Berkeley

Outline

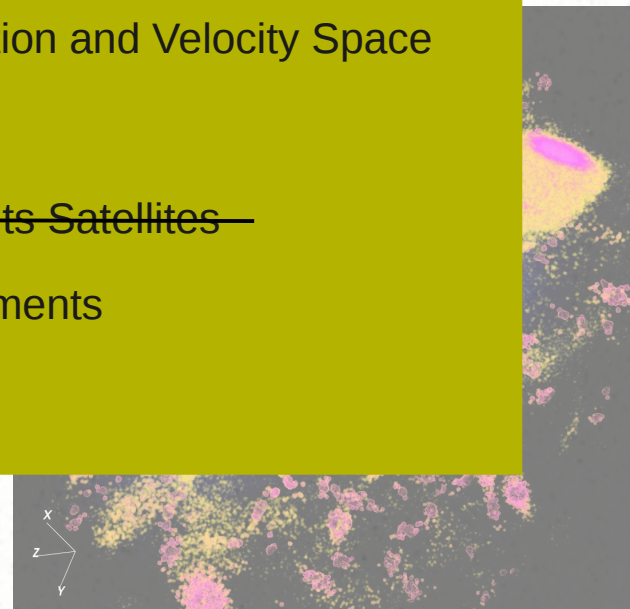
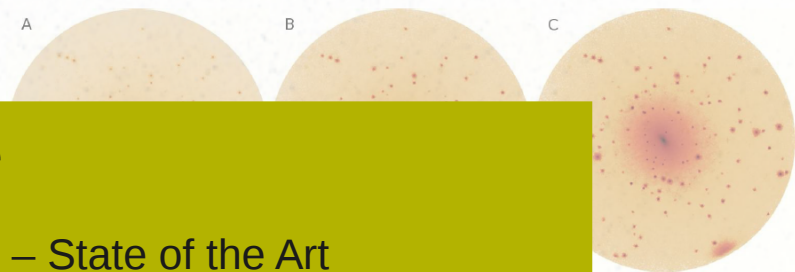
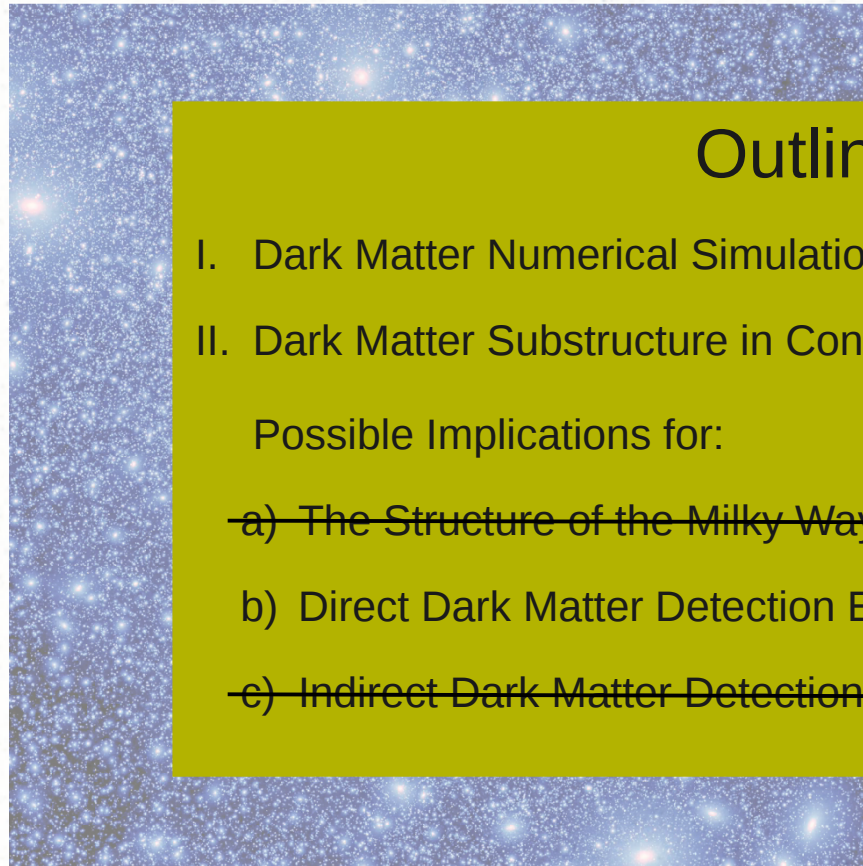
- I. Dark Matter Numerical Simulations – State of the Art
- II. Dark Matter Substructure in Configuration and Velocity Space

Possible Implications for:

- ~~a) The Structure of the Milky Way and its Satellites~~
- b) Direct Dark Matter Detection Experiments
- ~~c) Indirect Dark Matter Detection~~

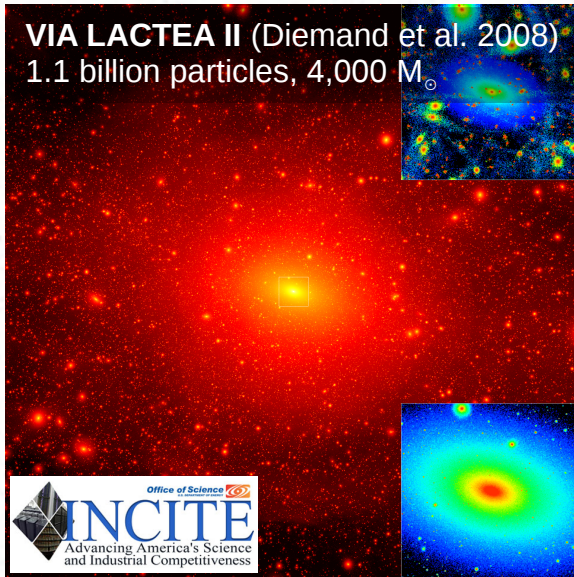
The Via Lactea collaboration

(P. Madau, J. Diemand, M. Zemp, B. Moore, J. Stadel, D. Potter, V. Rashkov)

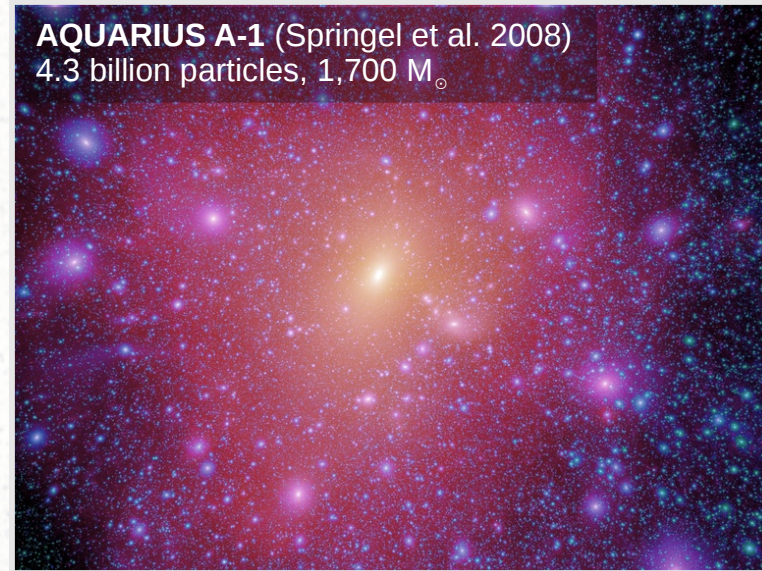


I. Dark Matter Simulations: The State Of The Art

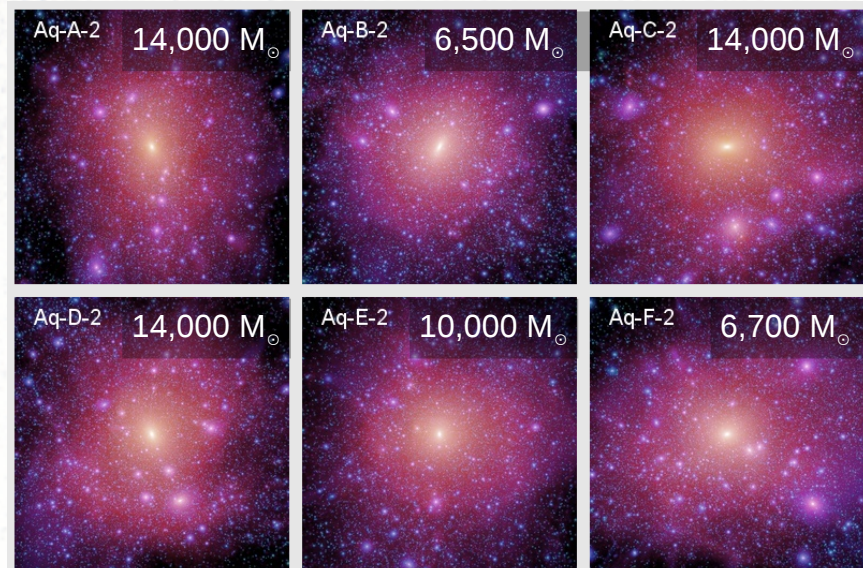
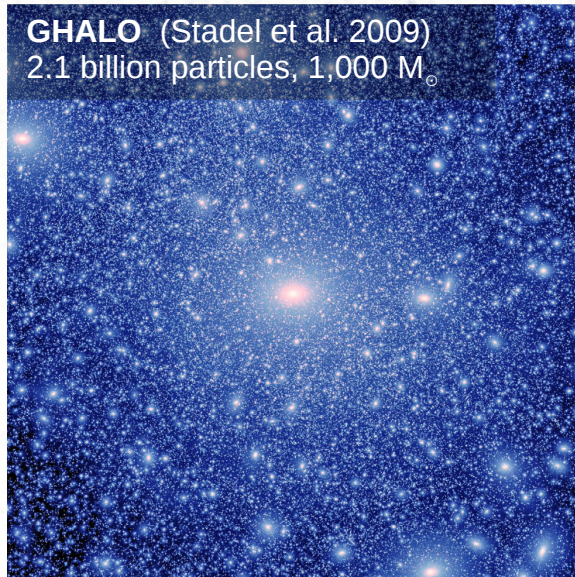
VIA LACTEA II (Diemand et al. 2008)
1.1 billion particles, 4,000 M_{\odot}



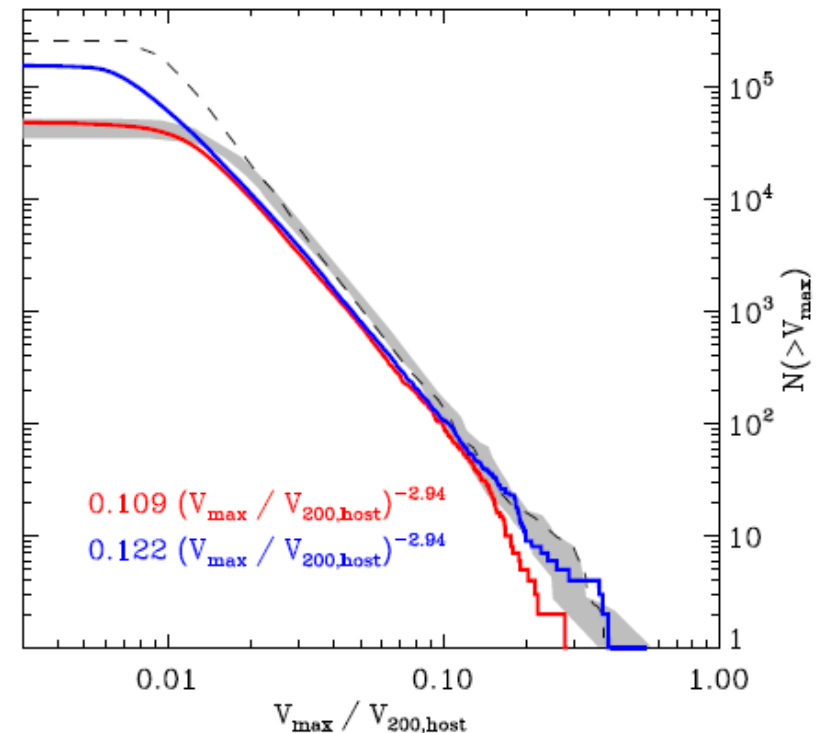
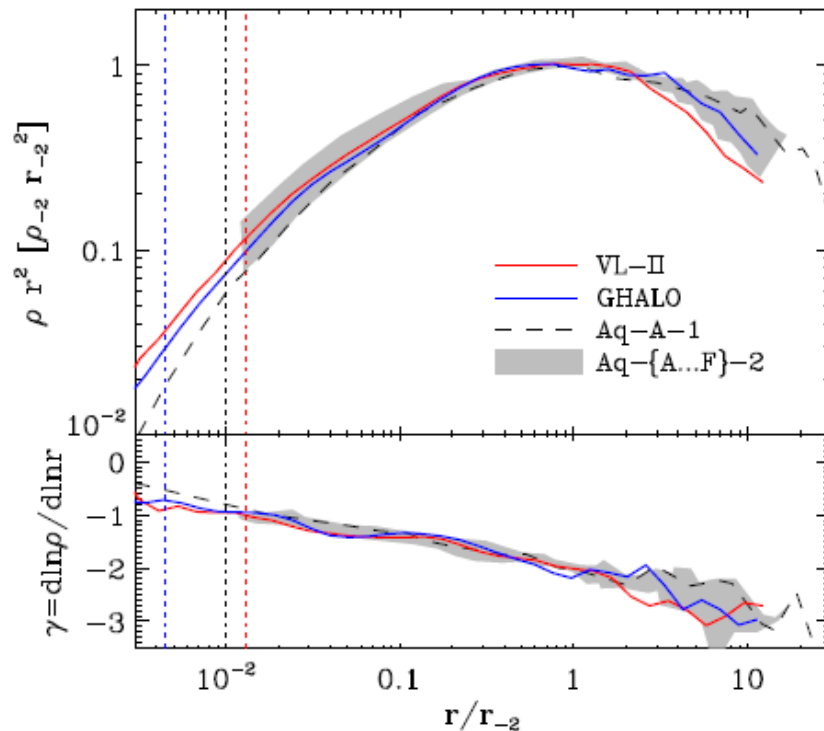
AQUARIUS A-1 (Springel et al. 2008)
4.3 billion particles, 1,700 M_{\odot}



GHALO (Stadel et al. 2009)
2.1 billion particles, 1,000 M_{\odot}



Via Lactea II/GHALO vs. Aquarius

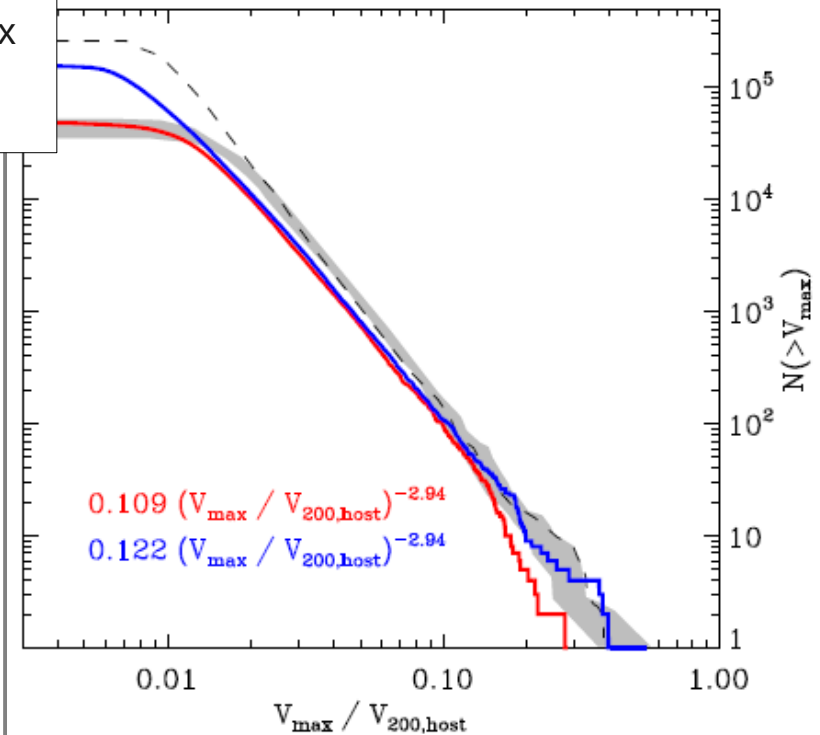
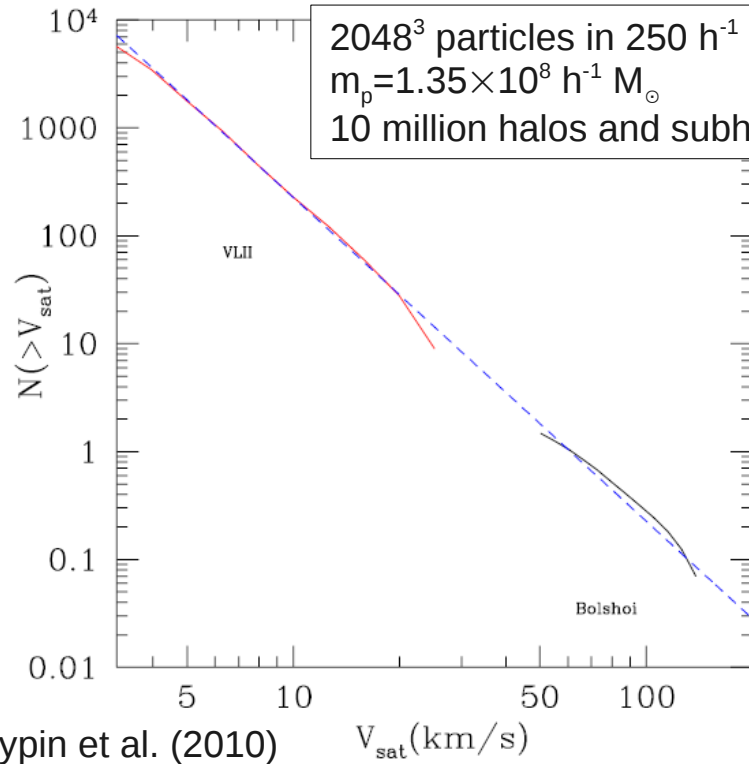


Via Lactea II, GHALO: **PKDGRAV2m**
 Aquarius: **Gadget-3**

Once appropriately scaled,
 VL-II, GHALO, and Aquarius
 agree with each other.

Via Lactea II/GHALO vs. Aquarius

Comparison with Bolshoi simulation

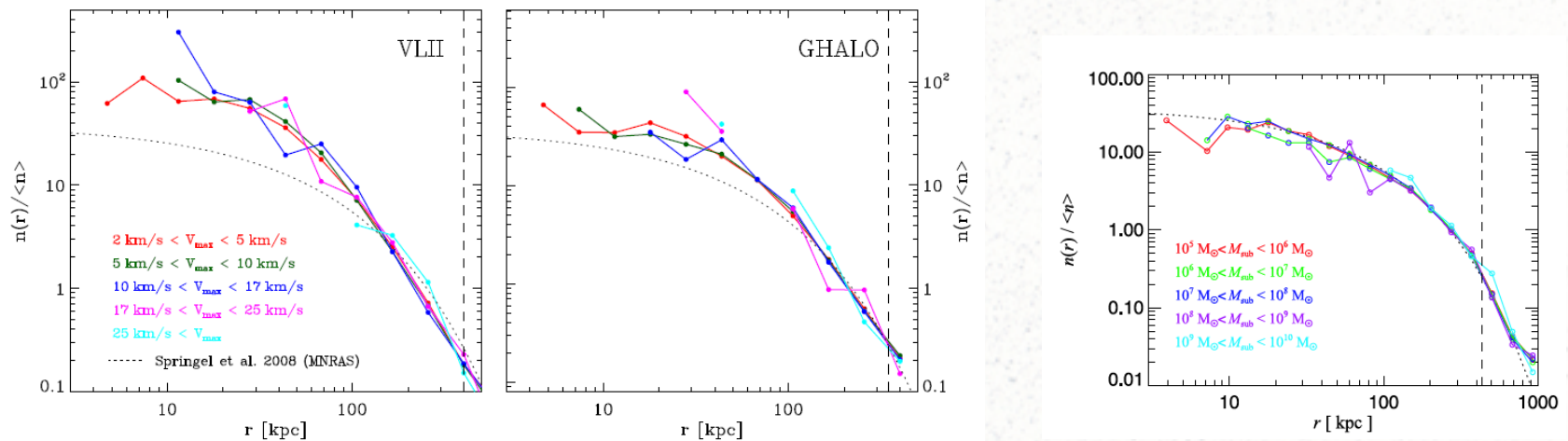


Via Lactea II, GHALO: **PKDGRAV2m**
Aquarius: **Gadget-3**

Once appropriately scaled,
VL-II, GHALO, and Aquarius
agree with each other.

Via Lactea II/GHALO vs. Aquarius

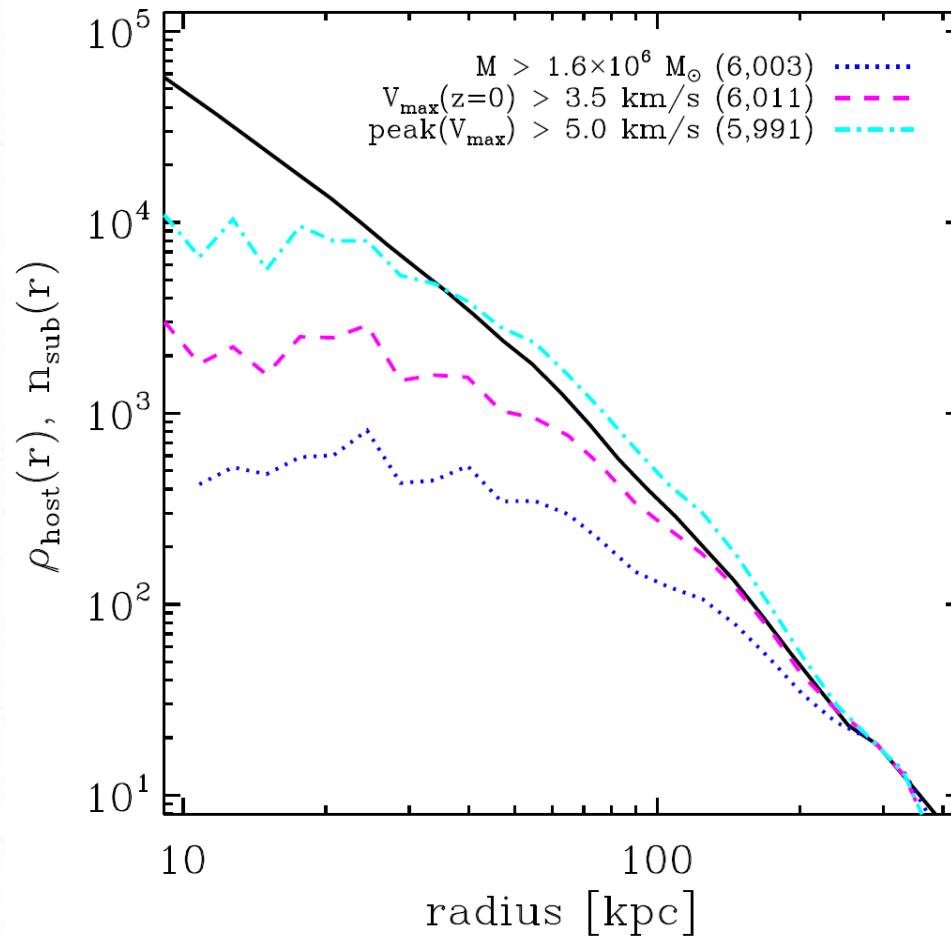
Some differences remain, e.g. in the radial distribution of subhalos.



Possible explanations:

- Slightly different cosmology? $\sigma_8=0.76$, $n_s=0.96$ in VL2/GHALO
 $\sigma_8=0.9$, $n_s=1$ in Aquarius
- Different subhalo finders? 6DFOF vs. SUBFIND
- Different sample selection? V_{\max} vs. M

The Radial Distribution of Subhalos Depends on Selection



The subhalo radial distribution is **anti-biased** with respect to the DM density: fewer subhalos in the center.

(cf. Ghigna et al. 2000; de Lucia et al. 2004)

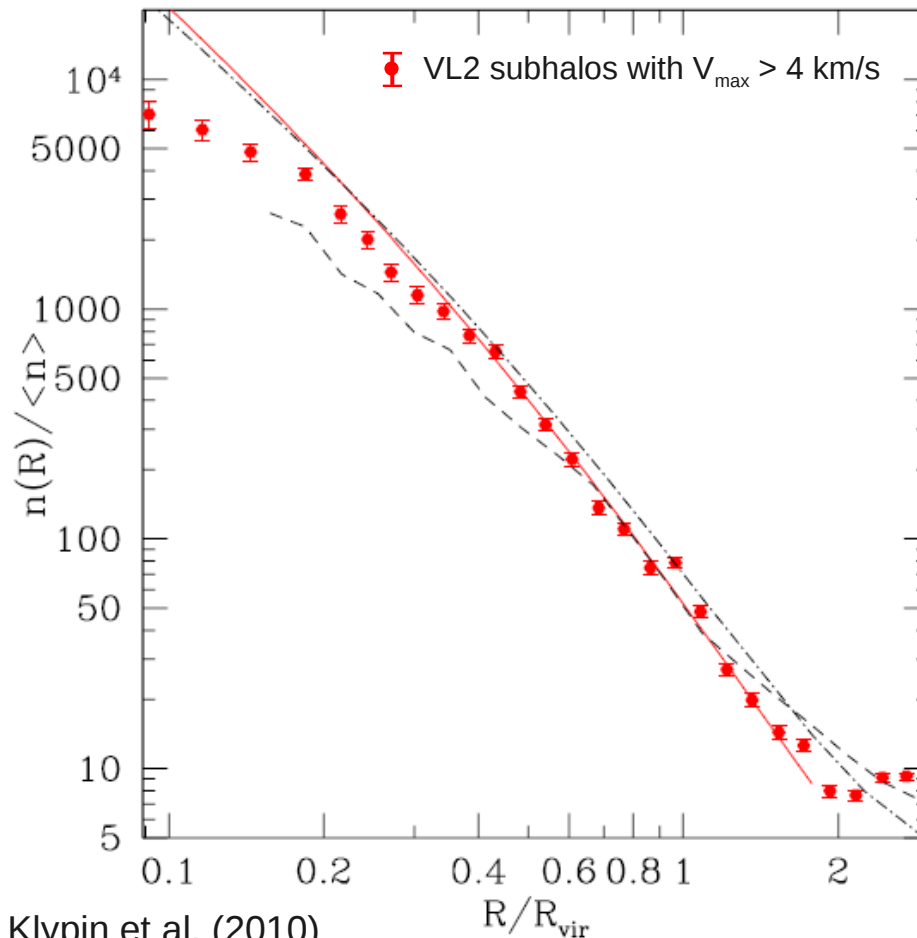
Depends on how one selection:

- strongest for $M(z=0)$ -selected,
- weaker for $V_{\text{max}}(z=0)$ -selected,
- disappears down to ~ 30 kpc for $\text{peak}(V_{\text{max}})$ -selected.

(cf. Nagai & Kravtsov 2005; Faltenbacher & Diemand 2006)

The Radial Distribution of Subhalos Depends on Selection

Subhalo $n(R)$ normalized with Bolshoi.



Klypin et al. (2010)

The subhalo radial distribution is **anti-biased** with respect to the DM density: fewer subhalos in the center.

(cf. Ghigna et al. 2000; de Lucia et al. 2004)

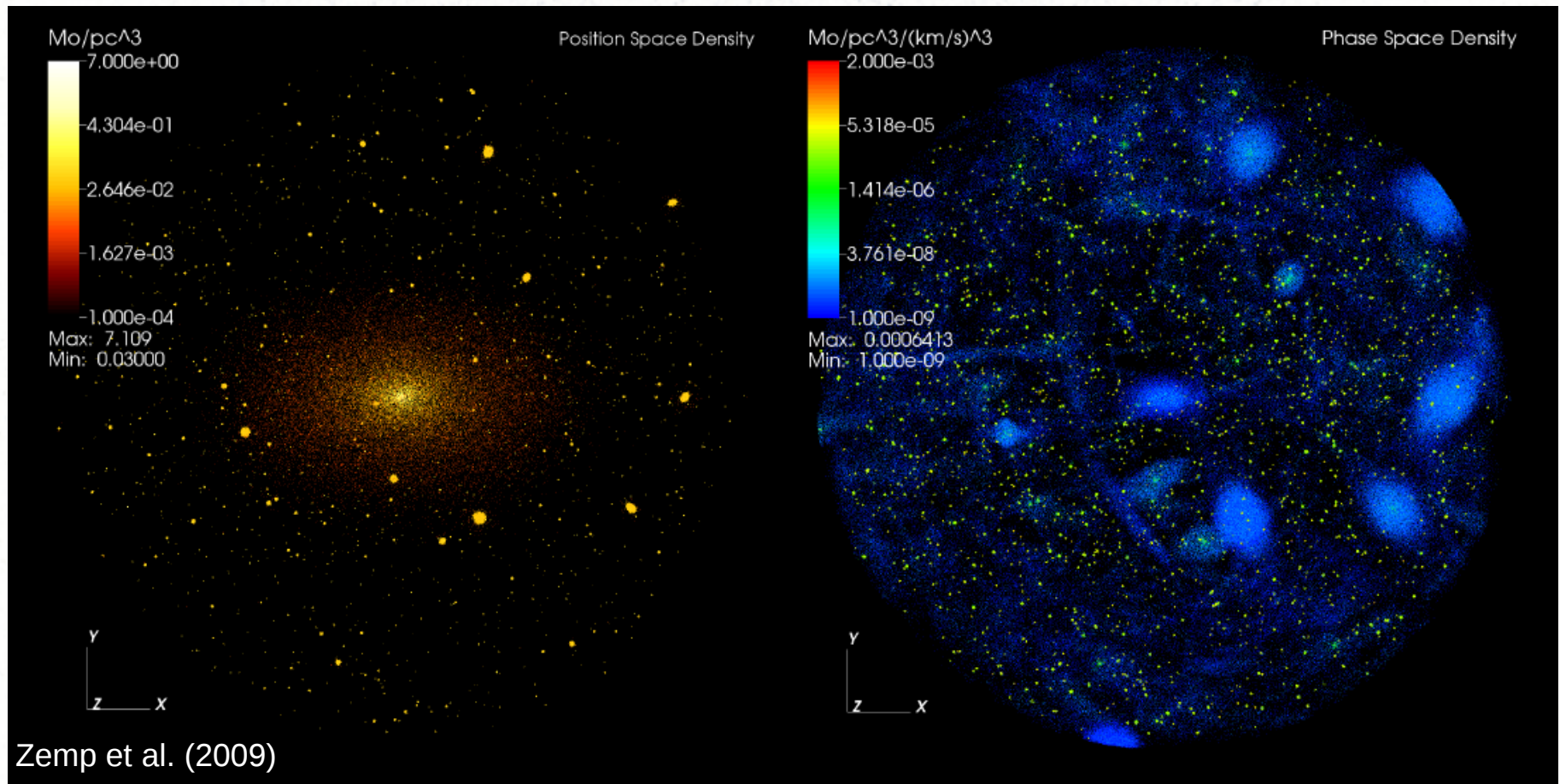
Depends on how one selection:

- strongest for $M(z=0)$ -selected,
- weaker for $V_{\text{max}}(z=0)$ -selected,
- disappears down to ~ 30 kpc for peak(V_{max})-selected.

(cf. Nagai & Kravtsov 2005; Faltenbacher & Diemand 2006)

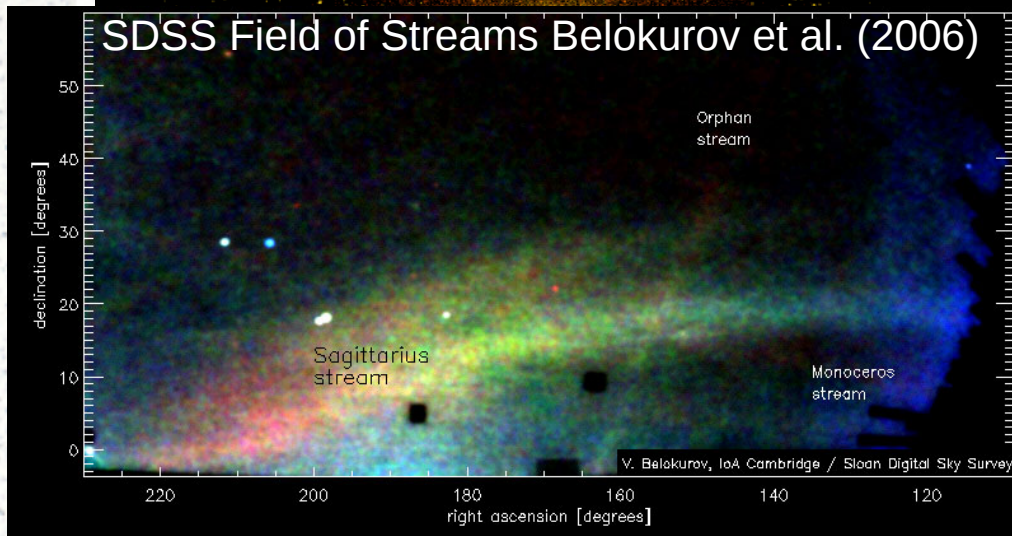
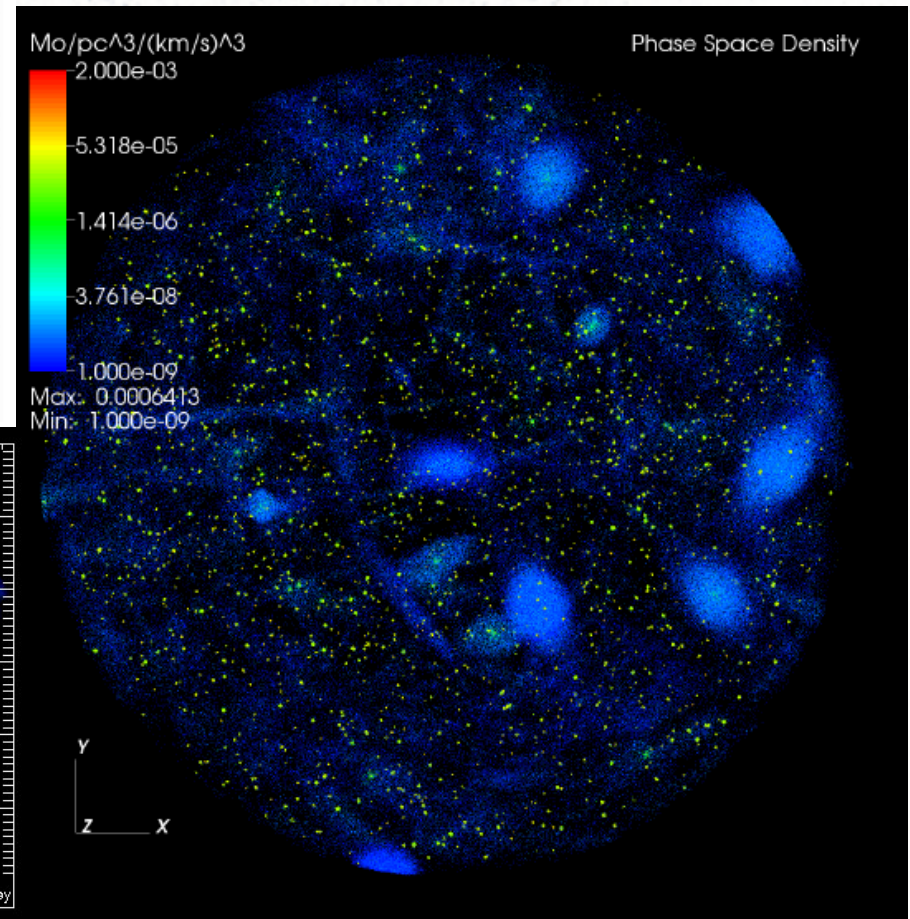
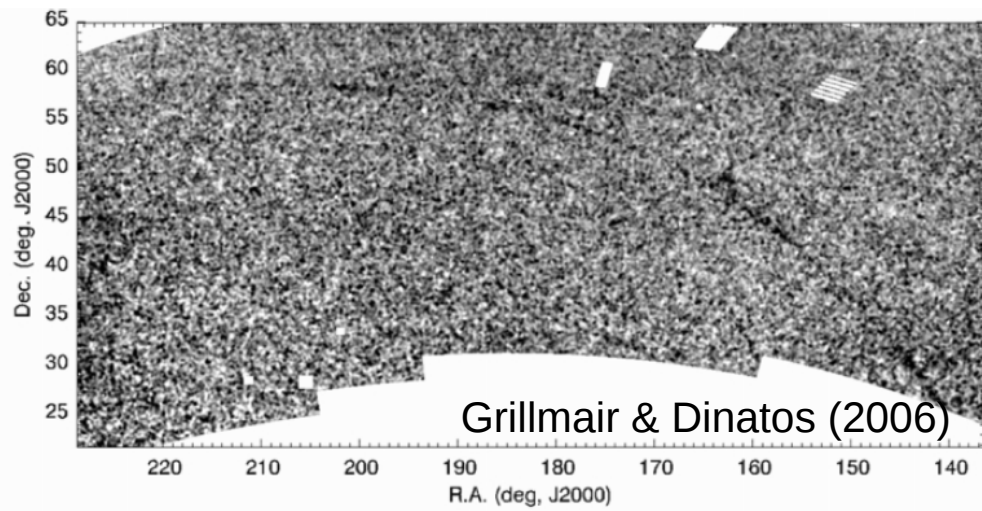
Velocity Space Substructure

Whereas previous simulations were almost completely smooth in the central region, with VL-II we resolve lots of subhalos and tidal streams even down to 8 kpc.



Velocity Space Substructure

Whereas previous simulations were almost completely smooth in the central region, tidal streams even down to 8 kpc.

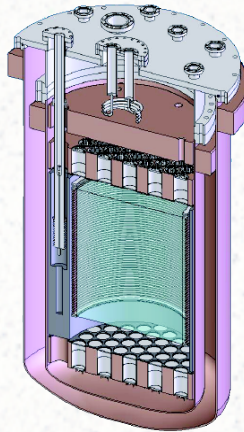


Substructure Relevance for Direct Detection

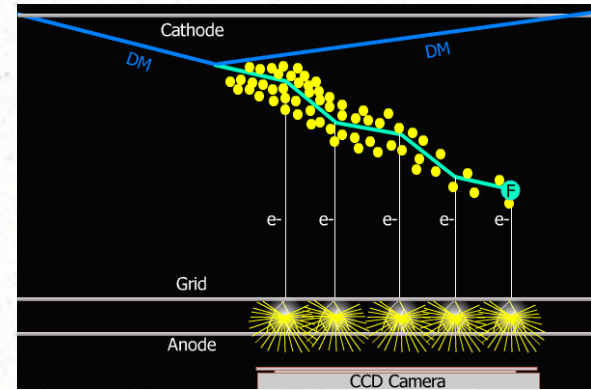
Cryogenic phonon detection
(e.g. CDMS)



Liquid Xenon scintillation
detectors (e.g. Xenon100, LUX)



Directionally sensitive
(e.g. DRIFT, DMTPC)



$$\frac{dR}{dE_R} = N_T M_N \frac{\rho_\chi \sigma_n}{2m_\chi \mu_{ne}^2} \frac{(f_p Z + f_n (A - Z))^2}{f_n^2} F^2[E_R] \int_{\beta_{min}}^{\infty} \frac{f(v)}{v} dv$$

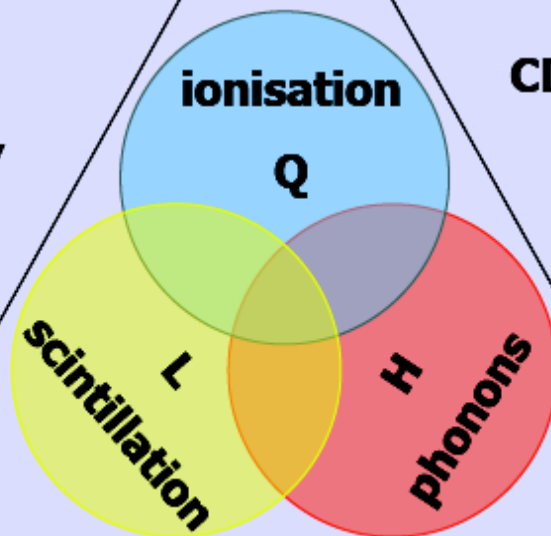
WIMP elastic nuclear recoils deposit $< 50\text{keV}$ of energy at a rate 10^{-6} to 2×10^{-2} event/day/kg

CoGeNT, DMTPC,
DRIFT1/II,
NEWAGE, MIMAC

\Rightarrow phonons, photons and charge whose relative proportions and /or characteristics depend on $dE/dx \Rightarrow$ particle type

ArDM, LUX, SIGN,
WARP, XENON10/100,
ZEPLIN II/III

CDMS, EDELWEISS,
SuperCDMS



ANAIS, CLEAN, DAMA,
DEAP, KIMS, LIBRA,
NAIAD, XMASS, ZEPLIN I

COUPP, CRESST I,
PICASSO, SIMPLE

High efficiency background rejection requires compound information and/or large self-shielding mass

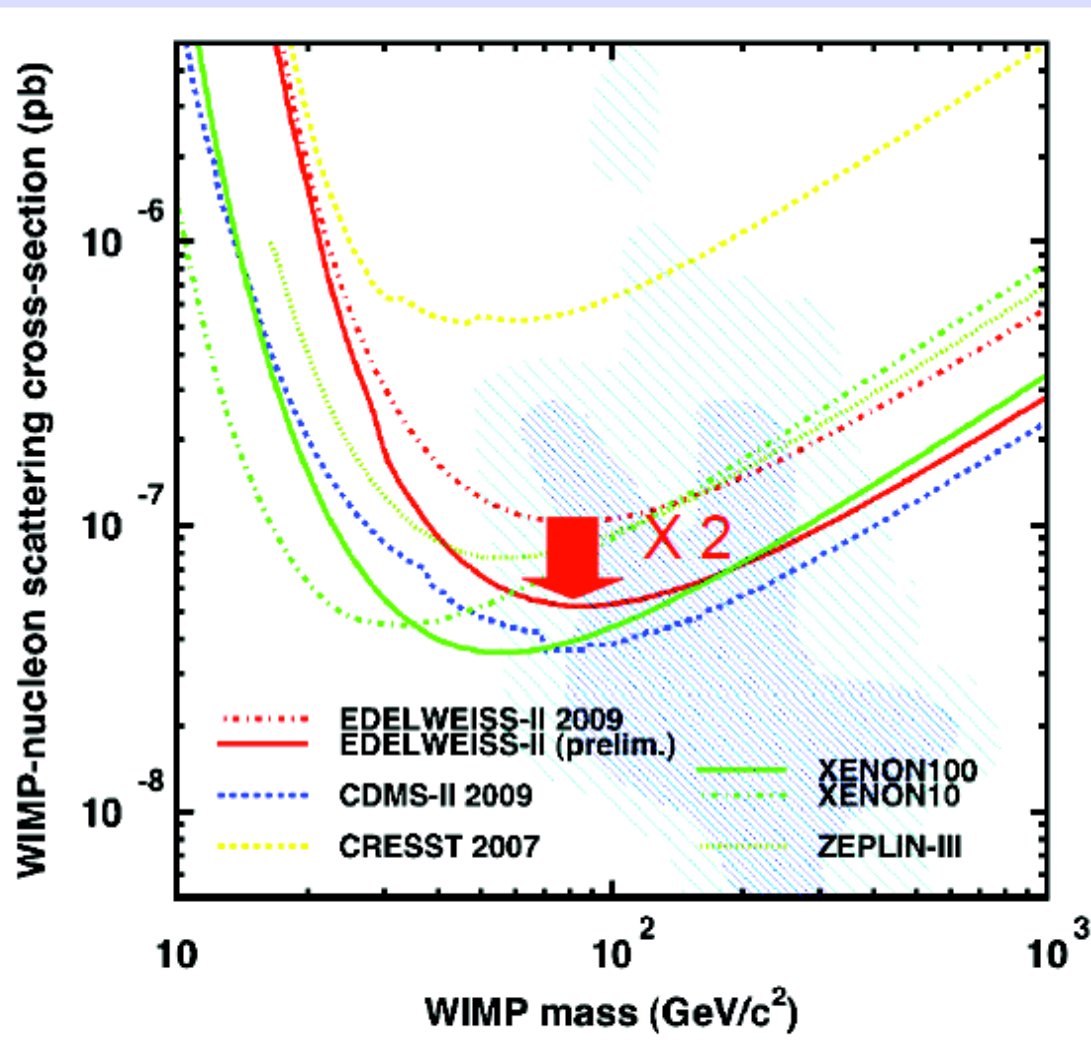
CRESST II,
ROSEBUD

World **competition** is intense and uses a wide range of **complementary** techniques

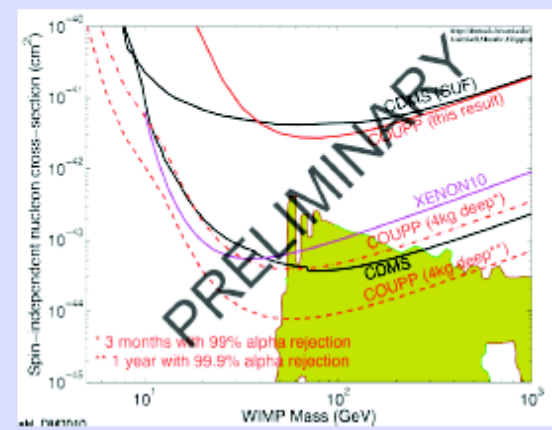


Current upper limits

Spin-independent

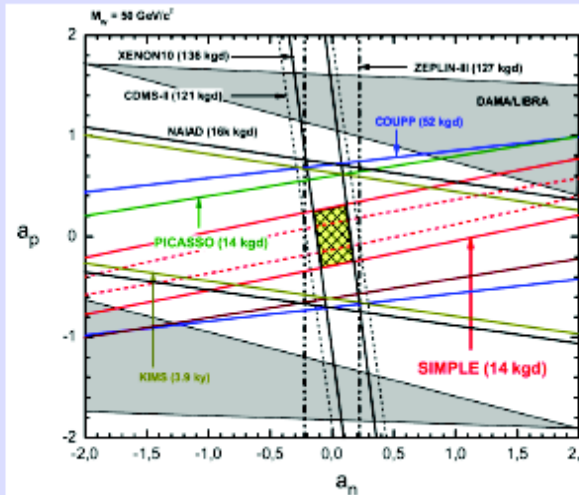
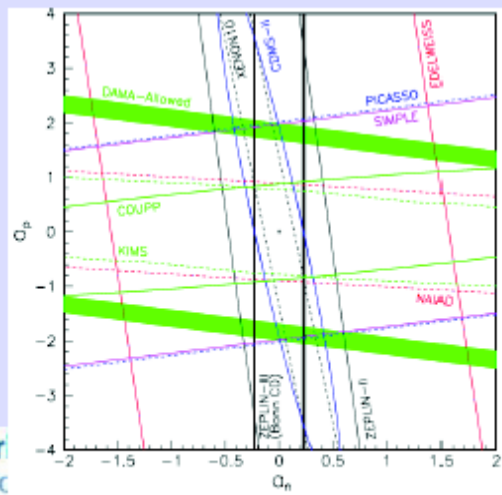
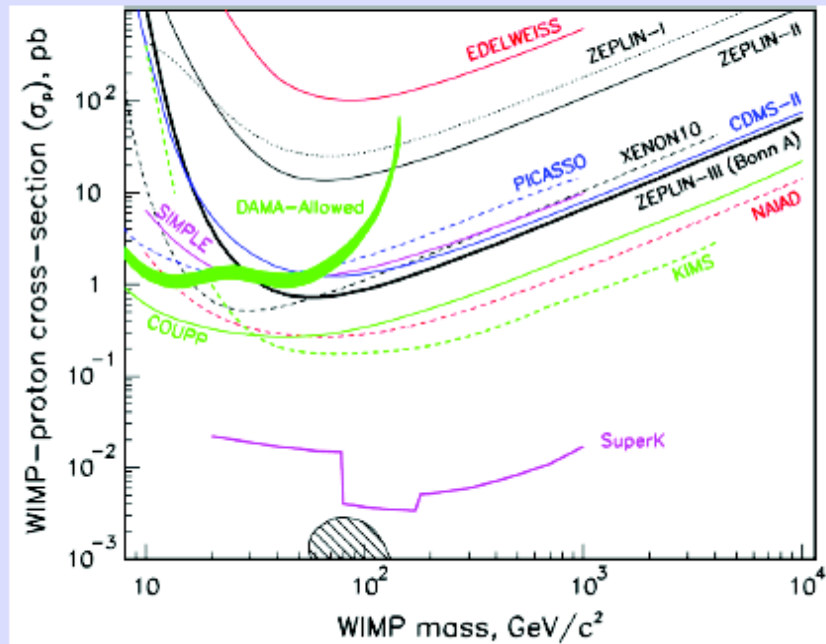
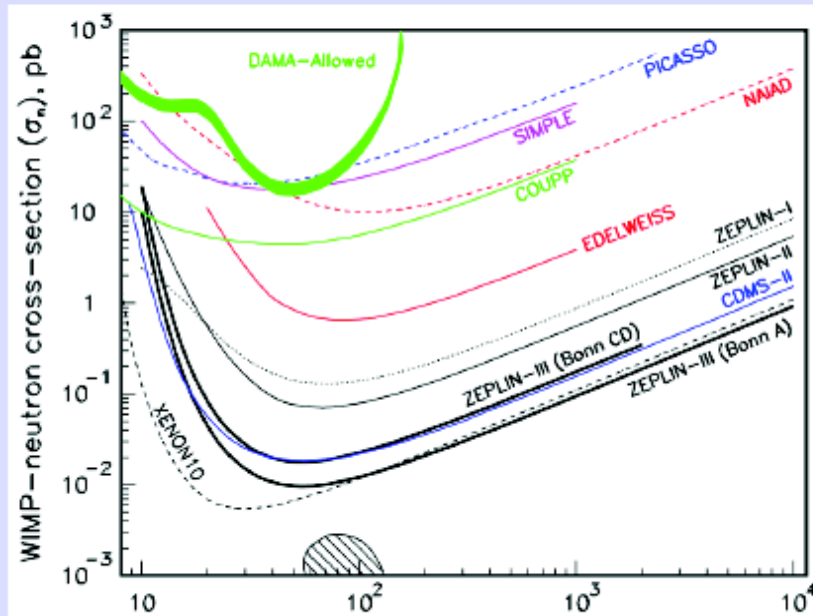


- DATA listed top to bottom on plot
- WARP 2.3L, 96.5 kg-days 55 keV threshold
- ZEPLIN II (Jan 2007) result
- CRESST 2007 60 kg-day CaWO4
- Edelweiss II first result, 144 kg-days interleaved Ge
- ZEPLIN III (Dec 2008) result
- XENON10 2007, measured σ_{eff} from Xe cube
- CDMS: Soudan 2004-2009 Ge
- ZEPLINIII (yr 3, with PMT upgrade) Proj. Sens.
- XENON100 projected sensitivity: 6000 kg-d, 5-30 keV, 45% eff.
- WARP 140kg (proj)
- LUX 300 kg LXe Projection (Jul 2007)
- Trotta et al 2008, CMSSM Bayesian: 68% contour
- Trotta et al 2008, CMSSM Bayesian: 95% contour
- Ellis et. al Theory region post-LEP benchmark points
- Baltz and Gondolo 2003
- Baltz and Gondolo, 2004, Markov Chain Monte Carlos



Current upper limits

Spin-dependent



Imperial College London

Imperial College - Cambridge - 6 August 2010

10

Slide from Tim Sumner's talk at the

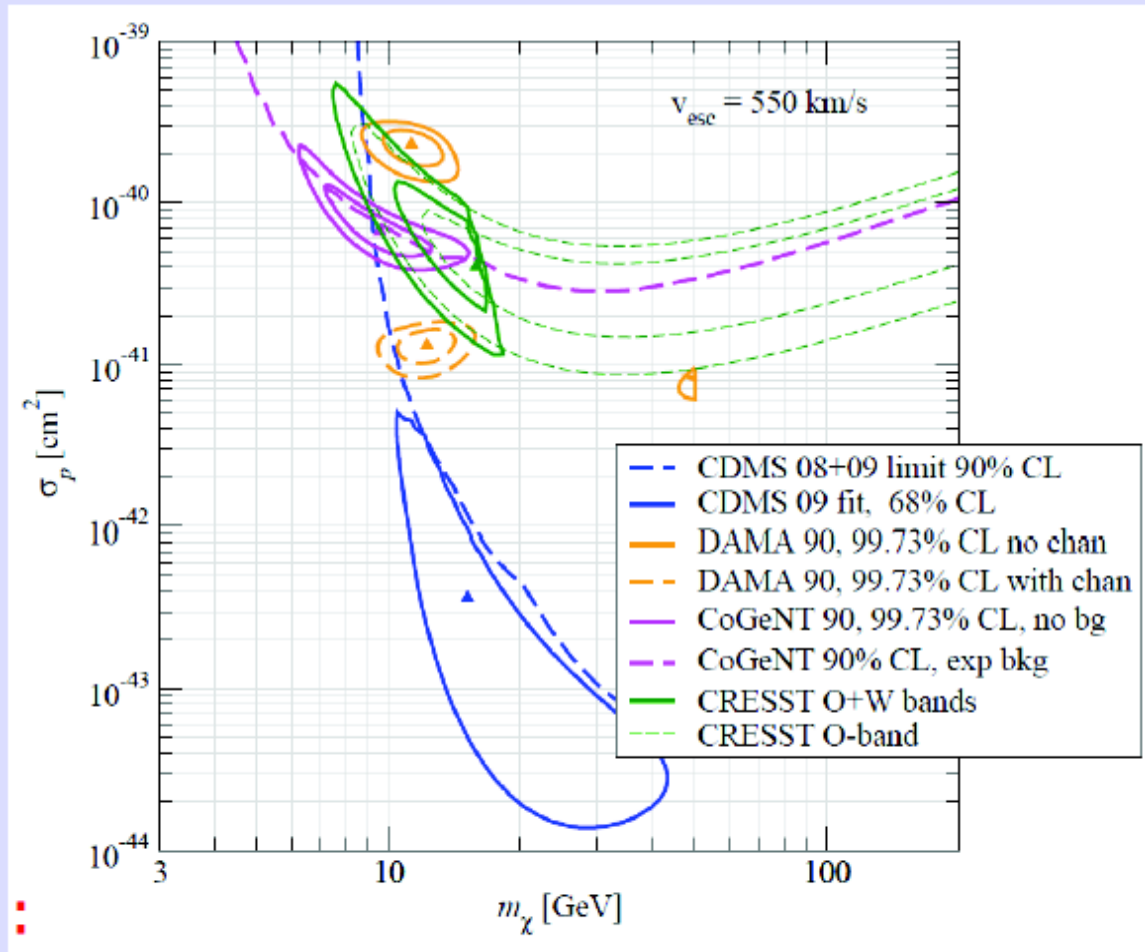
DARKNESS VISIBLE

conference in



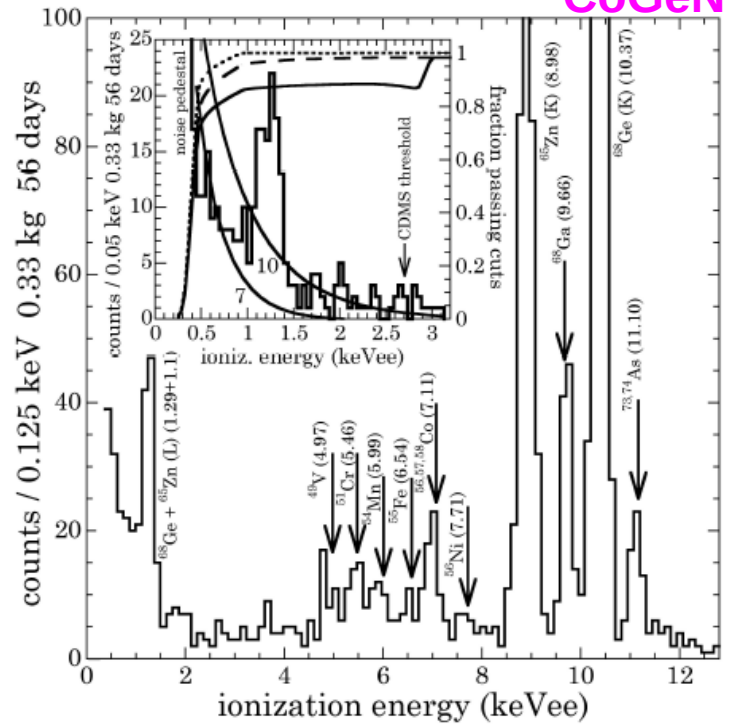
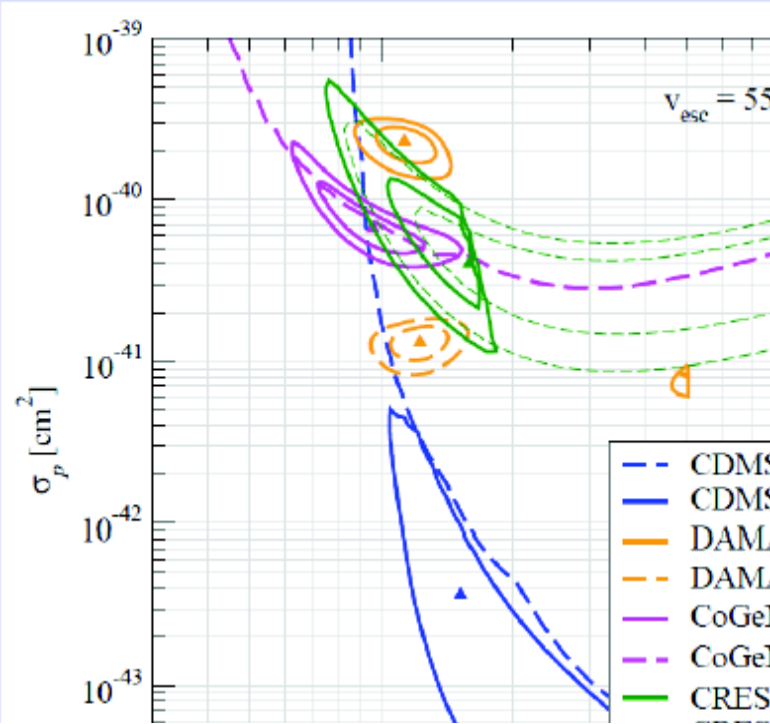
Low-mass WIMPs 5-50GeV (with no coupling to Z^0)

DAMA, CoGENT, CDMS, CRESST-II, XENON10/100



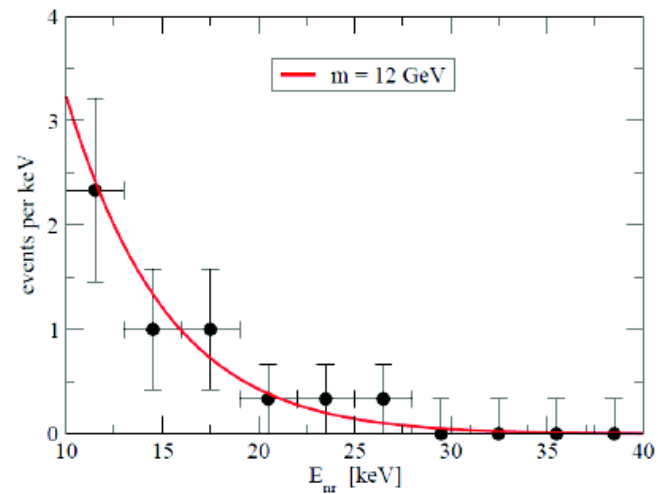
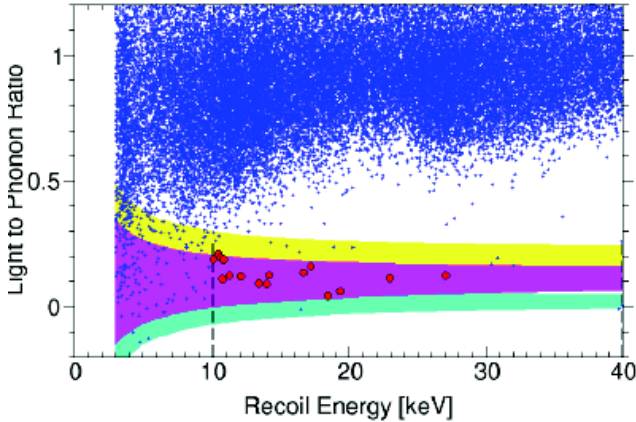
Low-mass WIMPs 5-50 GeV (with

DAMA, CoGeNT, CDMS, CRESST.



- CDMS 08+09 limit 90% CL
- CDMS 09 fit, 68% CL
- DAMA 90, 99.73% CL no chan
- DAMA 90, 99.73% CL with chan
- CoGeNT 90, 99.73% CL, no bg
- CoGeNT 90% CL, exp bkg
- CRESST O+W bands

CRESST



- Cambridge - 6 August 2010

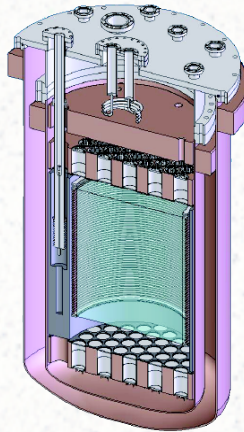
BLE conference in

Substructure Relevance for Direct Detection

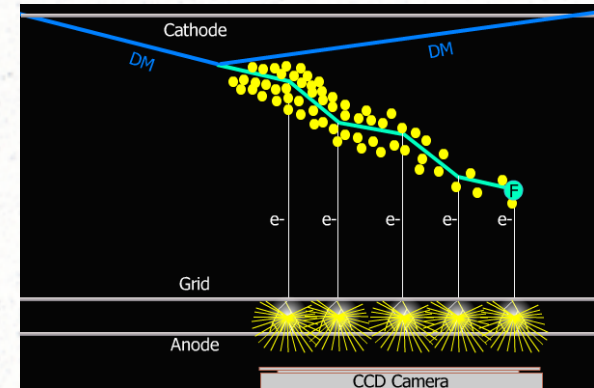
Cryogenic phonon detection
(e.g. CDMS)



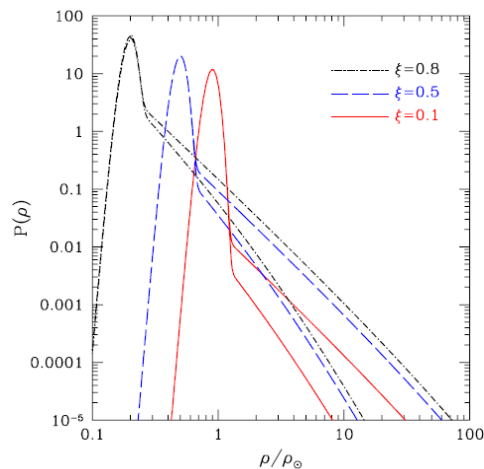
Liquid Xenon scintillation
detectors (e.g. Xenon100, LUX)



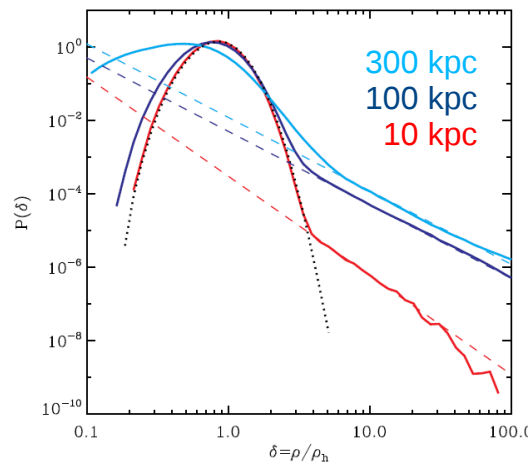
Directionally sensitive
(e.g. DRIFT, DMTPC)



$$\frac{dR}{dE_R} = N_T M_N \frac{\rho_\chi \sigma_n}{2m_\chi \mu_{ne}^2} \frac{(f_p Z + f_n (A - Z))^2}{f_n^2} F^2[E_R] \int_{\beta_{min}}^{\infty} \frac{f(v)}{v} dv$$



Kamionkowski & Koushiappas (2008)



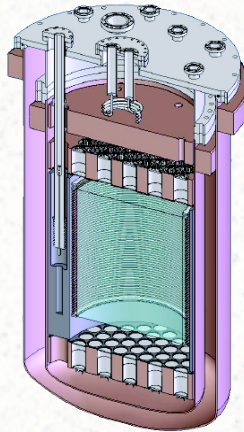
Kamionkowski, Koushiappas & MK (2010)
(see also Vogelsberger et al. 2009)

Substructure Relevance for Direct Detection

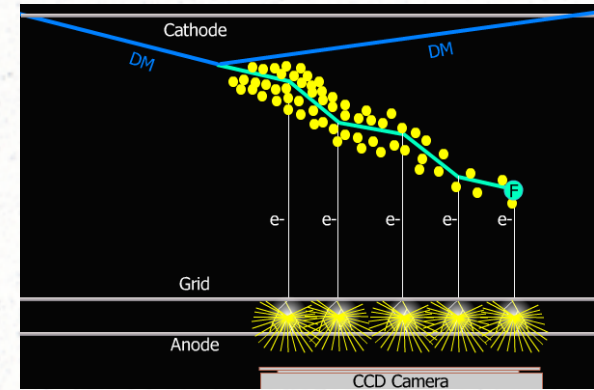
Cryogenic phonon detection
(e.g. CDMS)



Liquid Xenon scintillation
detectors (e.g. Xenon100, LUX)

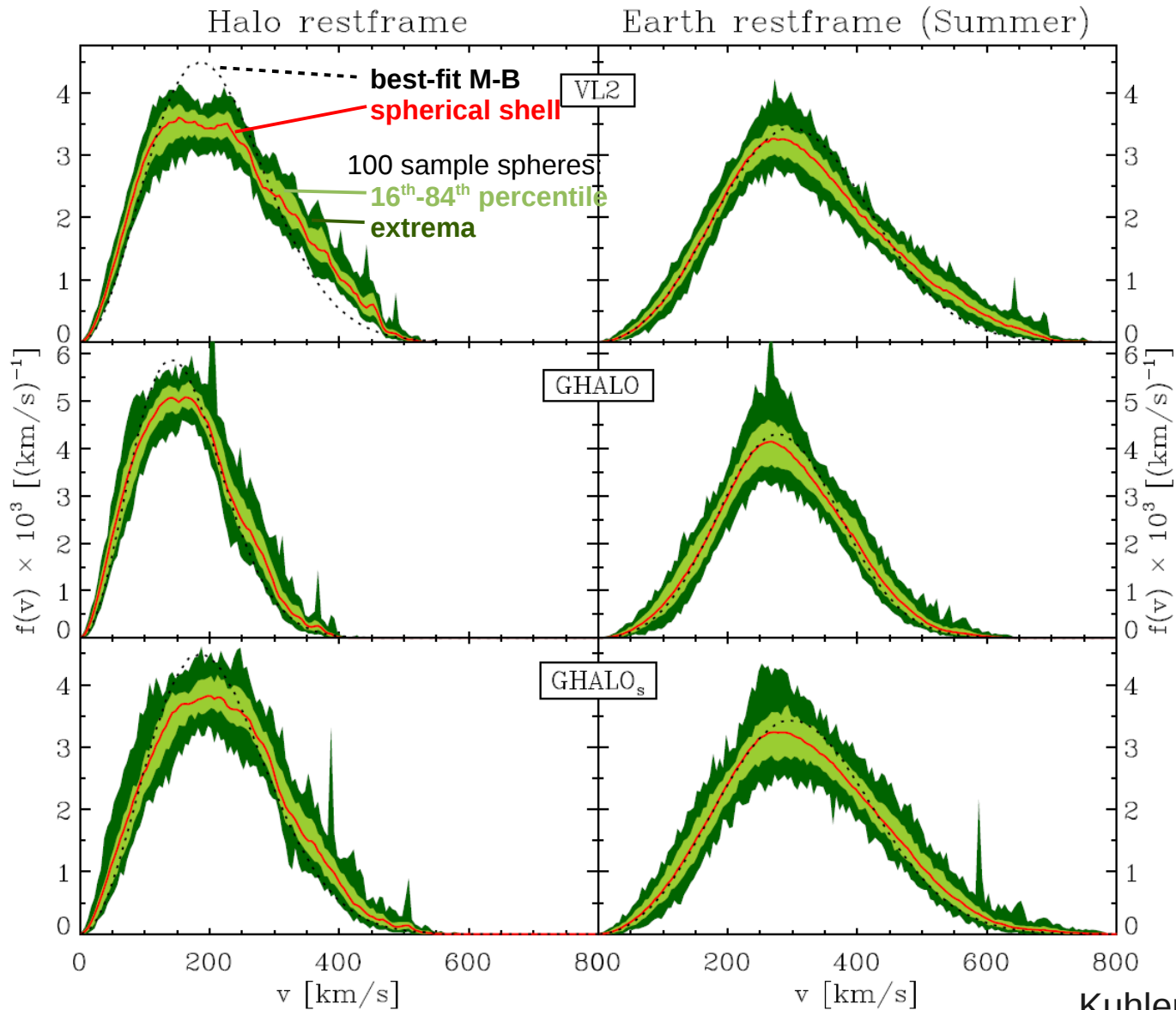


Directionally sensitive
(e.g. DRIFT, DMTPC)



$$\frac{dR}{dE_R} = N_T M_N \frac{\rho_\chi \sigma_n}{2m_\chi \mu_{ne}^2} \frac{(f_p Z + f_n (A - Z))^2}{f_n^2} F^2[E_R] \int_{\beta_{min}}^{\infty} \frac{f(v)}{v} dv$$

Velocity Space Substructure



Kuhlen et al. (2010)

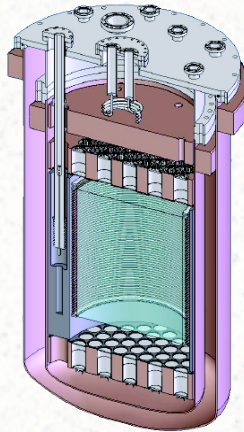
See also: Hansen et al. (2005), Vogelsberger et al. (2009)

Substructure Relevance for Direct Detection

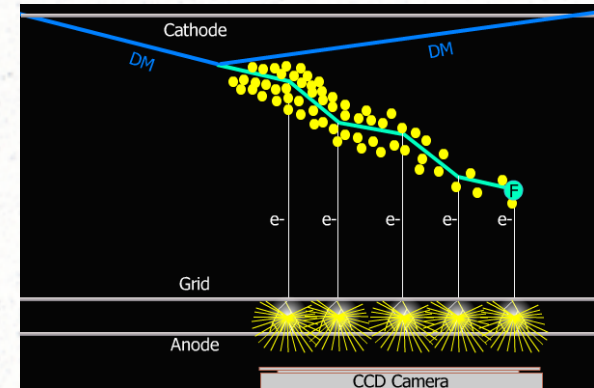
Cryogenic phonon detection
(e.g. CDMS)



Liquid Xenon scintillation
detectors (e.g. Xenon100, LUX)



Directionally sensitive
(e.g. DRIFT, DMTPC)



$$\frac{dR}{dE_R} = N_T M_N \frac{\rho_\chi \sigma_n}{2m_\chi \mu_{ne}^2} \frac{(f_p Z + f_n (A - Z))^2}{f_n^2} F^2[E_R] \int_{\beta_{\min}}^{\infty} \frac{f(v)}{v} dv$$

$$\beta_{\min} = \sqrt{\frac{1}{2m_N E_R} \left(\frac{m_N E_R}{\mu} + \delta \right)}$$

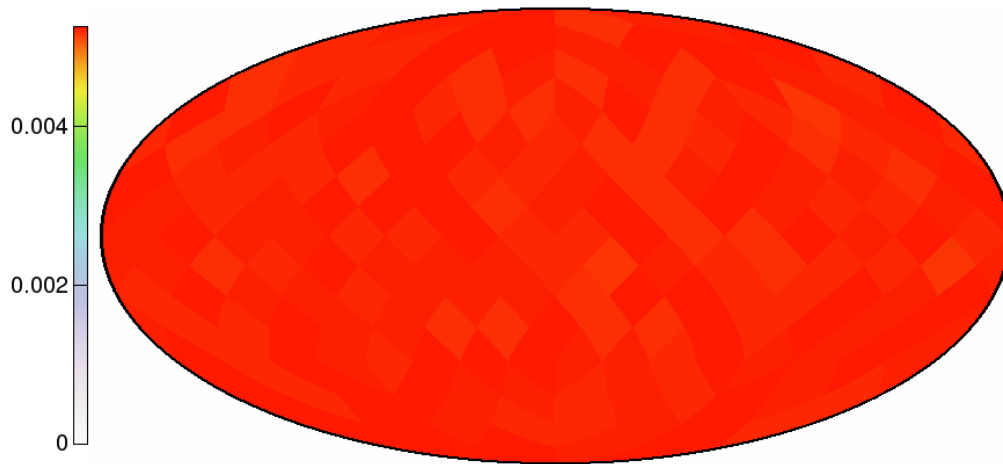
$f(v)$ is not Maxwellian!

Substructures can be important if β_{\min} is large.

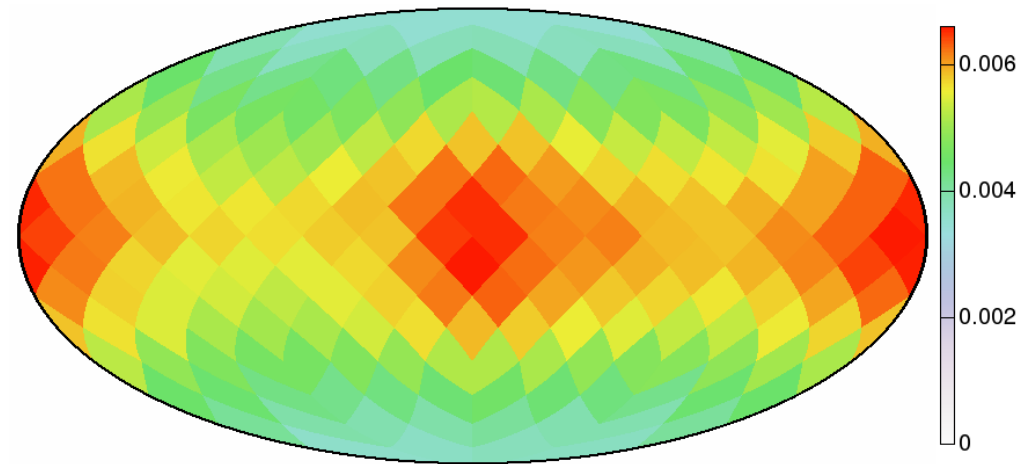
- Inelastic DM ($\delta > 0$)
- Light DM ($M_\chi < 10 \text{ GeV}$)
- Directionally sensitive experiments often require high E_{recoil} , large β_{\min} .

Velocity Direction in Halo Rest Frame

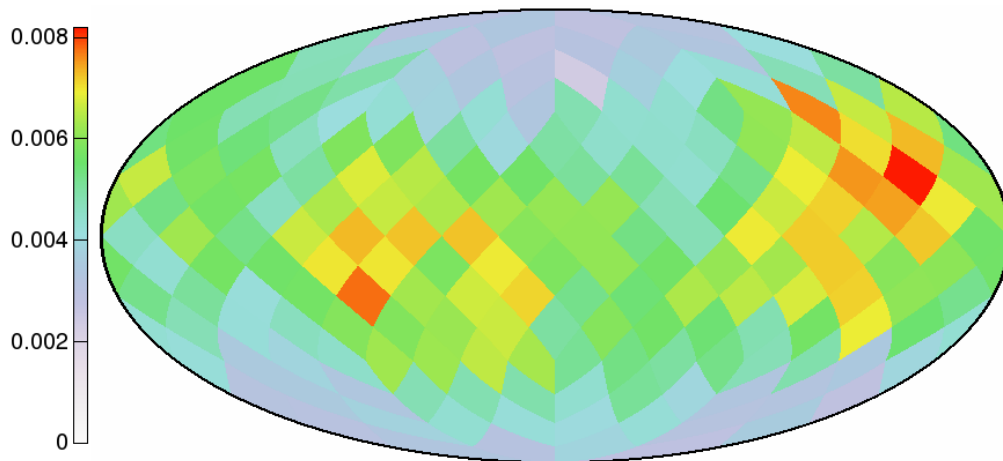
Maxwell-Boltzmann (isotropic)



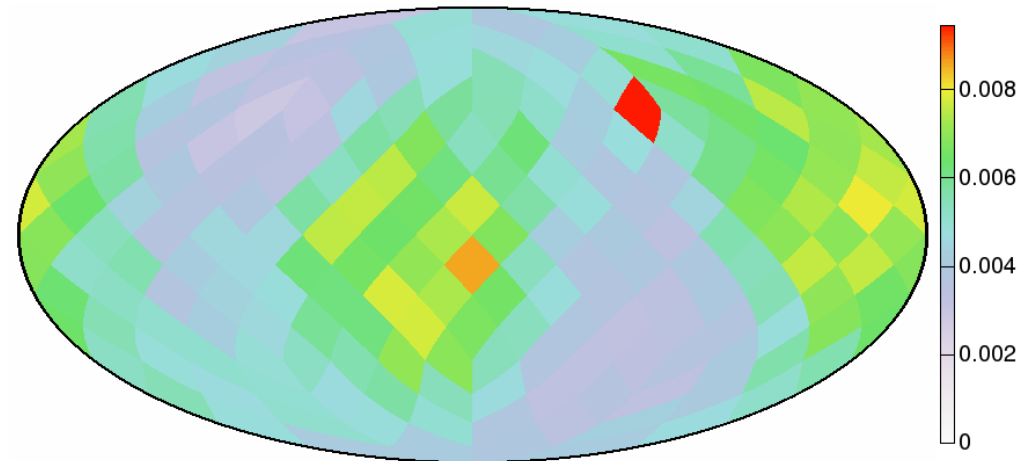
Spherical Shell ($8 \text{ kpc} < R < 9 \text{ kpc}$)



Sample Sphere #001

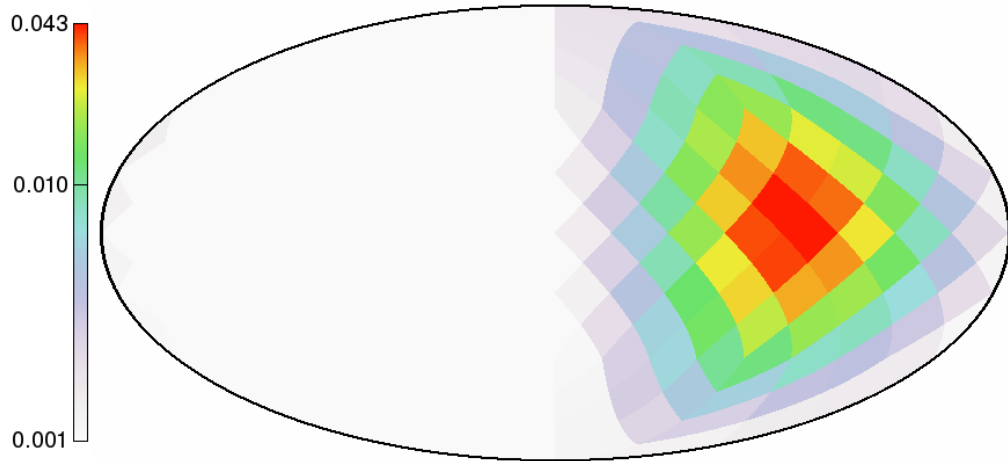


Sample Sphere #004 (containing a subhalo)

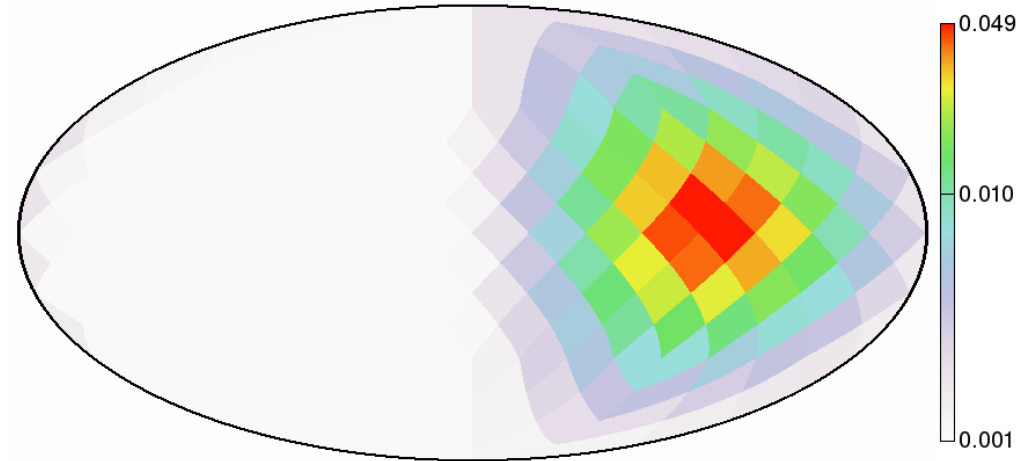


... in Earth Rest Frame $v_{\min} = 0$ km/s

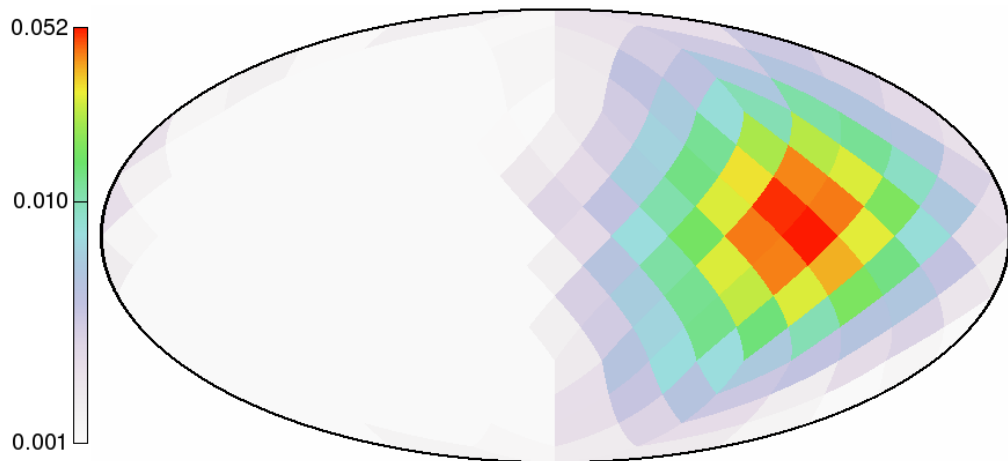
Maxwell-Boltzmann (isotropic)



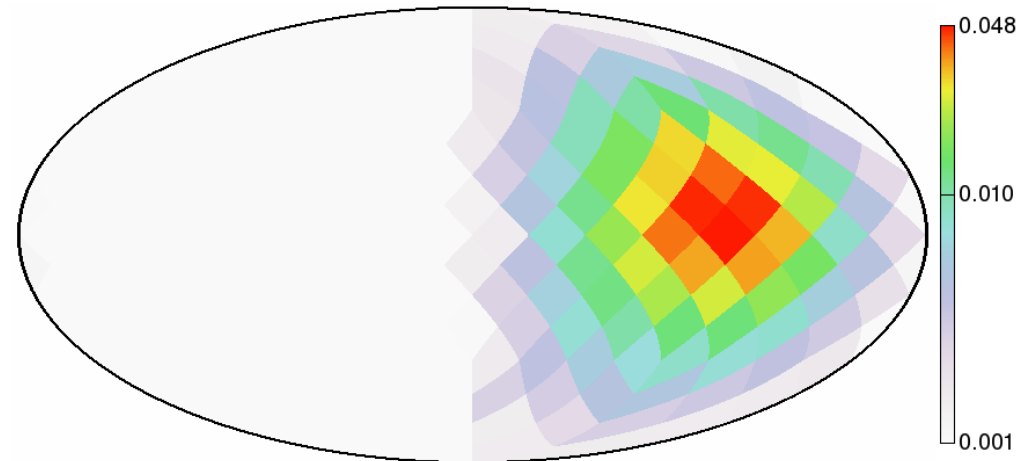
Spherical Shell (8 kpc < R < 9 kpc)



Sample Sphere #001

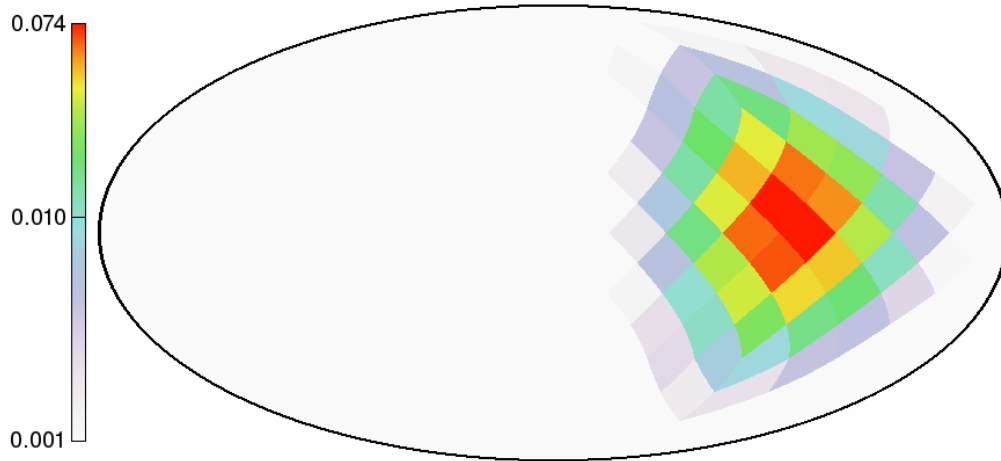


Sample Sphere #004 (containing a subhalo)

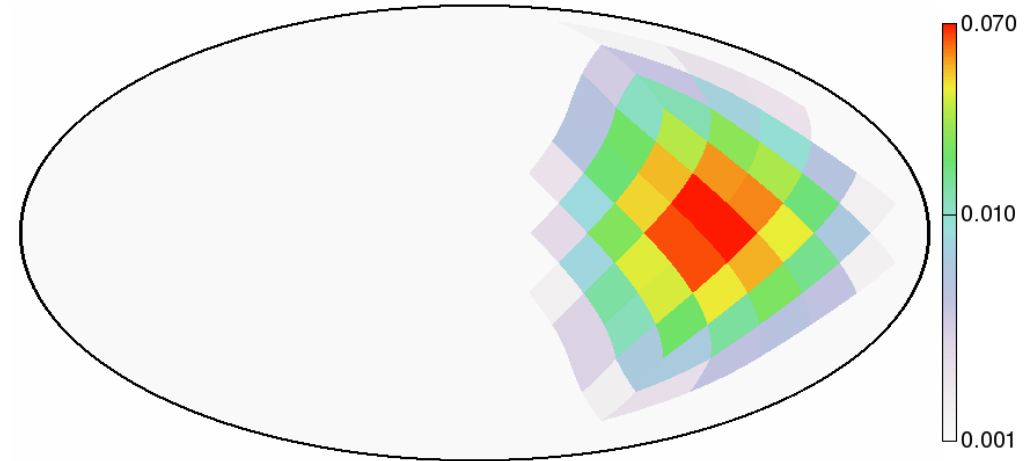


... in Earth Rest Frame $v_{\min} = 500$ km/s

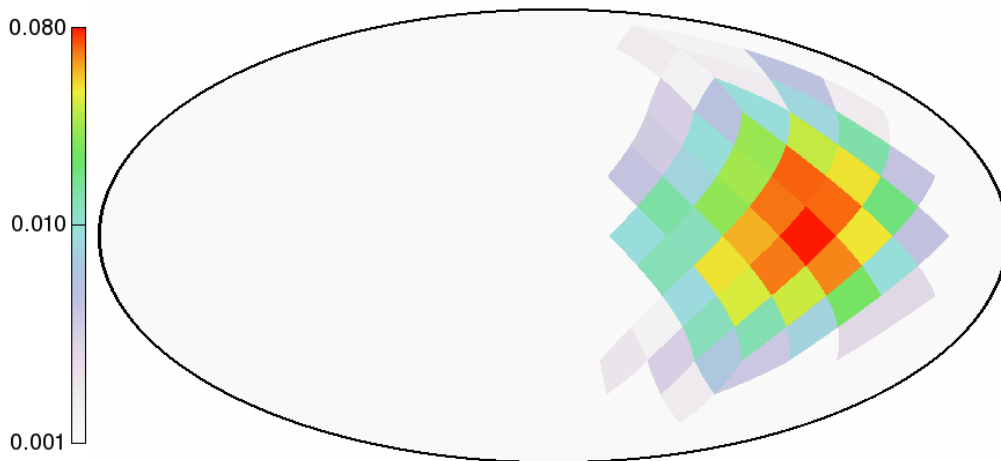
Maxwell-Boltzmann (isotropic)



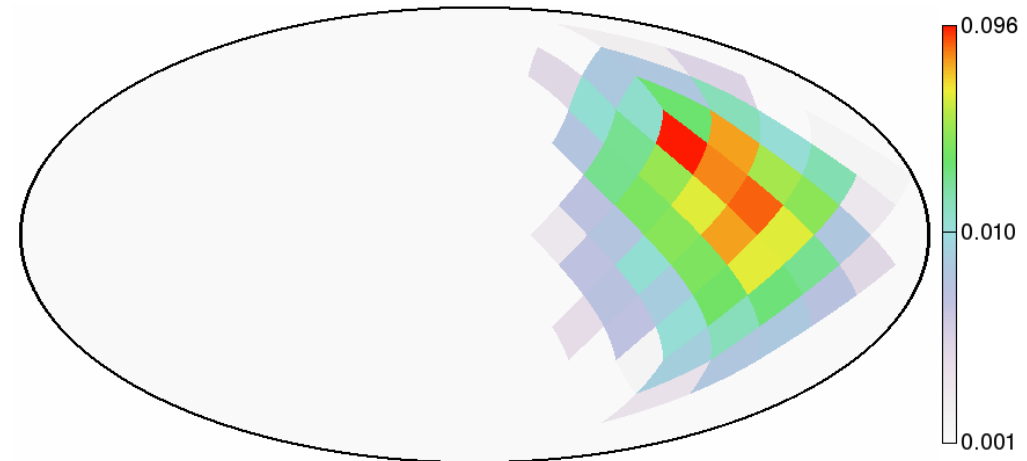
Spherical Shell (8 kpc < R < 9 kpc)



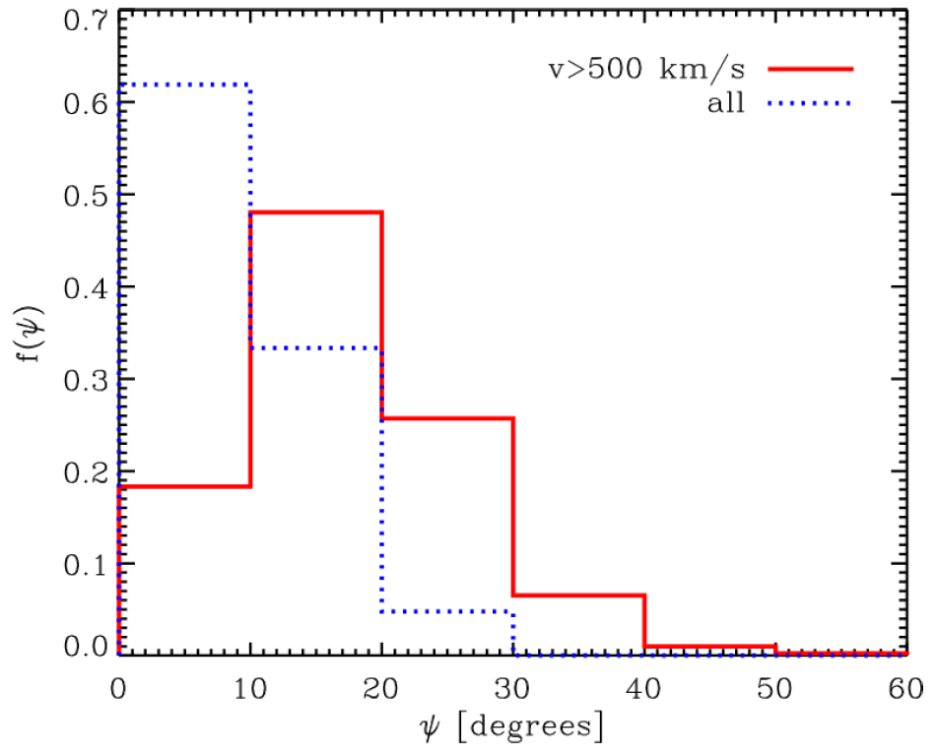
Sample Sphere #001



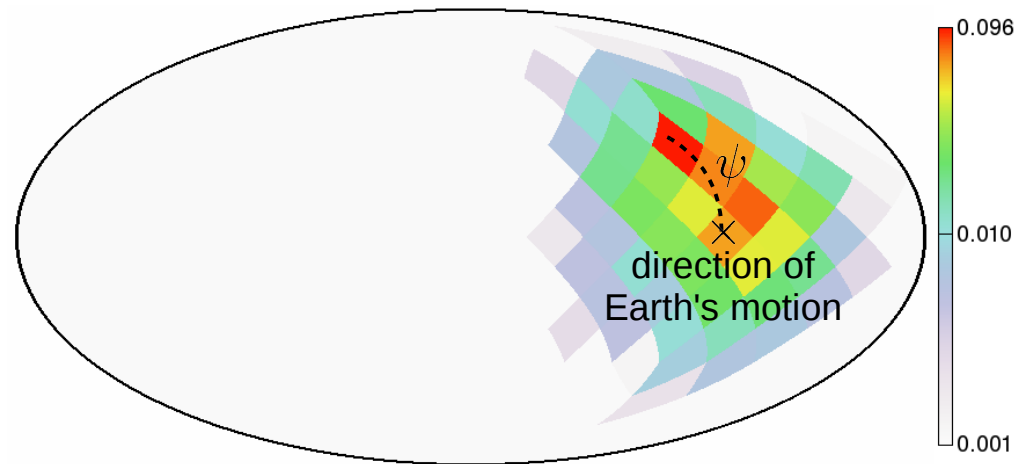
Sample Sphere #004 (containing a subhalo)



... in Earth Rest Frame $v_{\min} = 500$ km/s

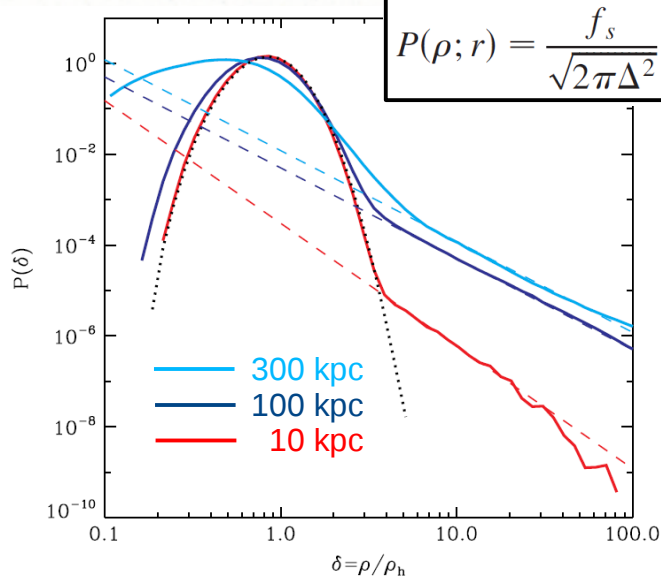


Sample Sphere #004 (containing a subhalo)



At $v_{\min} = 500$ km/s the hotspot is more than 10° away from the direction of Earth's motion in $\sim 80\%$ of all cases!

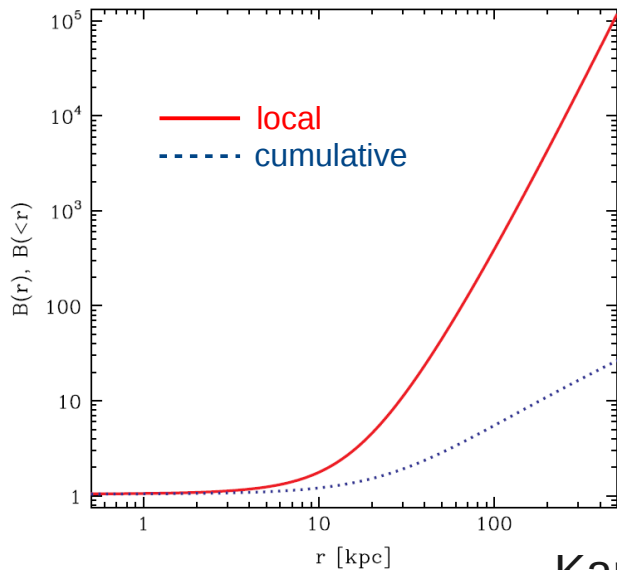
Substructure Boost Factor



$$P(\rho; r) = \frac{f_s}{\sqrt{2\pi}\Delta^2} \frac{1}{\rho} \exp\left\{-\frac{1}{2\Delta^2} \left[\ln\left(\frac{\rho}{\rho_h} e^{\Delta^2/2}\right)\right]^2\right\} + (1 - f_s) \frac{1 + \alpha(r)}{\rho_h} \Theta(\rho - \rho_h) \left(\frac{\rho}{\rho_h}\right)^{-(2+\alpha)}$$

- We measure the PDF of ρ/ρ_{host} in the simulation.
- It's fit well by a **log-normal** plus a **powerlaw** tail due to substructure.

$$\alpha \approx 0.0 \pm 0.1 \quad 1 - f_s(r) = 7 \times 10^{-3} \left(\frac{\bar{\rho}(r)}{\bar{\rho}(r = 100 \text{ kpc})}\right)^{-0.26}$$



$$B(r) = \frac{\int \rho^2 dV}{\int [\bar{\rho}(r)]^2 dV} = \int_0^{\rho_{\text{max}}} P(\rho, r) \frac{\rho^2}{[\bar{\rho}(r)]^2} d\rho$$

$$B(r) = f_s e^{\Delta^2} + (1 - f_s) \frac{1 + \alpha}{1 - \alpha} \left[\left(\frac{\rho_{\text{max}}}{\rho_h}\right)^{1-\alpha} - 1 \right]$$

Local boost (e.g. at 8 kpc or at the G.C.) \neq Total boost

Kamionkowski, Koushiappas & Kuhlen (2010)

Conclusions

- The number of subhalos resolved in the to-date largest simulations (Via Lactea II, GHALO, Aquarius) is ever increasing: >300,000 at latest count.
- The simulations indicate copious DM velocity substructure from subhalos and tidal streams. Corresponding stellar streams are being discovered: will there be a Missing Streams Problem?
- Velocity substructure in the DM distribution function might noticeably affect DM direct detection experiments, especially for DM models or experimental setups that are sensitive to high velocity DM particles: e.g. inelastic DM, light DM, directionally sensitive experiments.
- At high velocities (>500 km/s) the direction of incoming DM particles is more than 10° away from the direction of Earth's motion in ~80% of all cases!
- The annihilation boost factor from substructure depends on radius: at the GC or at the Sun it's not likely to be important.